

Multistability in chiral cavity-polariton systems

S. S. Gavrilov,^{1,*} A. V. Sekretenko,¹ N. A. Gippius,^{2,3} C. Schneider,⁴
S. Höfling,⁴ M. Kamp,⁴ A. Forchel,⁴ and V. D. Kulakovskii¹

¹*Institute of Solid State Physics RAS, Chernogolovka, 142432, Russia*

²*A. M. Prokhorov General Physics Institute, RAS, Moscow 119991, Russia*

³*LASMEA, UMR 6602 CNRS, Université Blaise Pascal, 63177 Aubière, France*

⁴*Technische Physik, Physikalisches Institut and Wilhelm Conrad Röntgen Research Center for Complex Material Systems, Universität Würzburg, D-97074 Würzburg, Germany*

(Dated: November 18, 2018)

Chirality of cavity polaritons, brought on by lifted degeneracy of right- and left-circularly polarized polariton levels, makes possible a new kind of multistability that manifests itself in fast (few tens of picoseconds) spin-flip transitions in the cavity field under a resonant pump with fixed polarization but varying intensity. This effect is due to resonance-shifting polariton-polariton interactions; it has been described within a coherent mean-field approach and observed experimentally using pulsed 70 picosecond long excitation in a magnetic field.

PACS numbers: 71.36.+c, 42.65.Pc

Collective phenomena in cavity-polariton systems are attracting a broad interest within the last decade. Being weakly interacting bosons formed due to strong exciton-photon coupling in microcavities [1], polaritons exhibit collective properties typical of both matter waves and light waves, including optic parametric scattering [2].

Spin-dependent polariton-polariton interaction [3, 4] gives rise to a multistability effect making a resonantly driven mode able to be switched between distinct “stability branches” [5]. Such switchings are typically accompanied by sharp jumps in the cavity-field intensity and polarization, though being caused by even slight changes of external conditions nearby bifurcation points. The multistability imparts a strong hysteresis to the optic response of a microcavity and is considered as a base for a new generation of optical devices, such as memory elements [6] and logic gates [7] operating on micrometer and picosecond scales. Such very short times, giving cavity-polariton systems an advantage over electronic devices, stem from the short intrinsic lifetime of polaritons ($\lesssim 10$ ps) that is comparable to the lifetime of cavity photons. The repulsive interaction between polaritons is strong enough to blue-shift their energy by a value several times larger than their spectral linewidth, which results in large amplification factors attained in multistability induced transitions [8, 9].

By now the multistability of cavity-polariton systems has been observed under continuous-wave excitation, resulting in sharp transitions and pronounced hysteresis in the cavity transmission intensity and polarization [8–10]. In addition, several marked phenomena were observed, including many-mode optical parametric oscillation [11, 12], spin ring patterns [8, 9, 13], and polariton solitons [14], which all would be impossible without polariton bi- or multistability.

In this Letter we show that a lifted degeneracy of σ^\pm polariton modes makes possible a new mechanism of the

cavity-field spin-flip transformation due to varying pump power, even with fixed pump polarization. This effect is impossible in conventional (non-chiral) cavities, neither can it take place in bistable VCSEL-based devices. In fact, the considered phenomenon reveals the distinction of polariton multistability caused by the amplitude dependence of resonance frequency, in contrast to optical multistability related to the nonlinearity of gains or decay rates (e.g. [15]) like that in VCSELs ([16, 17]) or semiconductor lasers.

The σ^\pm splitting of polariton levels can be provided by the splitting in either the photonic or excitonic component. The first way has recently been implemented in cavities with special asymmetric mask patterns [18]. On the other hand, the exciton levels can be split due to the Zeeman effect [19]. In our work we have employed the latter way and performed time- and polarization-resolved studies of the cavity transmission in a magnetic field.

Multistability and steady-state solutions.—Resonantly driven cavity-polariton systems are usually considered within a coherent mean-field approach based on Gross-Pitaevskii equations. For simplicity we write them for the single lower polariton mode driven by a coherent pump with zero in-plane wave vector ($\mathbf{k} = 0$) [5]:

$$i\hbar \frac{d}{dt} \begin{pmatrix} \psi_+ \\ \psi_- \end{pmatrix} = \begin{pmatrix} \hat{E}_0 - i\hat{\gamma}_0 \end{pmatrix} \begin{pmatrix} \psi_+ \\ \psi_- \end{pmatrix} + \begin{pmatrix} (V_1|\psi_+|^2 + V_2|\psi_-|^2)\psi_+ \\ (V_2|\psi_+|^2 + V_1|\psi_-|^2)\psi_- \end{pmatrix} + \begin{pmatrix} F_+(t) \\ F_-(t) \end{pmatrix}. \quad (1)$$

Herein are $F_\pm(t) = \sqrt{\frac{I_p(t)}{2}}(1 \pm \rho_p)e^{i(E_p/\hbar)t + i\phi_\pm}$; $I_p = |F_+|^2 + |F_-|^2$ the pump intensity, ρ_p the degree of circular polarization, E_p the pump energy, and $\Phi_p = \phi_+ - \phi_-$ the phase shift between the σ^\pm components of the pump wave. $V_{1,2}$ are the polariton-polariton interaction constants. The polariton mode is characterized by its energy \hat{E}_0 and decay rate $\hat{\gamma}_0$ which are 2×2 matrices written

in the σ^\pm basis. For simplicity we assume $\hat{\gamma}_0$ to be spin-symmetric, $\hat{\gamma}_0 = \gamma_0 \hat{1}$, whereas \hat{E}_0 has the form

$$\hat{E}_0 = E_0 \hat{1} + \frac{\delta_c}{2} \begin{pmatrix} 1 & 0 \\ 0 & -1 \end{pmatrix} + \frac{\delta_l}{2} \begin{pmatrix} 0 & 1 \\ 1 & 0 \end{pmatrix}. \quad (2)$$

Its first term is the energy of polaritons in a symmetric structure, the second term provides the σ^\pm splitting, $E_0^+ - E_0^- = \delta_c$, and the third term gives the X-Y splitting $E_0^{(x)} - E_0^{(y)} = \delta_l$ in the Cartesian basis $\begin{pmatrix} \psi_x \\ \psi_y \end{pmatrix} = \frac{1}{\sqrt{2}} \begin{pmatrix} 1 & 1 \\ i & -i \end{pmatrix} \begin{pmatrix} \psi_+ \\ \psi_- \end{pmatrix}$. The X-Y splitting coming from the exciton part may be due to crystalline disorder, or it can be introduced manually by applying stress [20] along one of the structure axes; the same effect can be due to TE-TM splitting of cavity photons at $\mathbf{k} \neq 0$.

The interaction between cross-circularly polarized polaritons (V_2) is attractive and typically much weaker than that between polaritons with the same circular polarization (V_1) [21–23]; below we assume $V_2 = -0.1V_1$. The units for ψ can be fixed by the condition $V_1 = 1$, so that $|\psi|^2$ has the dimension of energy and, in the case of circularly polarized excitation, coincides with the blue-shift of the driven mode. In the following simulations we set $\gamma_0 = 0.05 \text{ meV}$ and $\Delta = E_p - E_0 = 0.2 \text{ meV}$.

By substituting $\psi_\pm(t) = \bar{\psi}_\pm e^{-i(E_p/\hbar)t}$ into Eq. (1) one gets a time-independent equation that allows one to find the response of the driven mode on a constant pump, $\bar{\psi}_\pm = \bar{\psi}_\pm(I_p, \rho_p, \Phi_p)$. The problem concerned with asymptotic stability of the steady-state solutions was considered in Ref. [24].

In the simplest case of a degenerate system ($\delta_{c,l} = 0$) under purely circular excitation ($\rho_p = 1$), the dependence of the steady-state cavity-field intensity on pump intensity takes the form of an ‘S’-shaped circuit [25, 26] (Fig. 1a). This implies, first, the possibility of a jump (“switch-up”) in the cavity transmission and, second, the hysteresis of the response under slowly changing pump power. As long as $|V_2| \ll V_1$, the response of the system excited with elliptically polarized light may be treated in terms of the two S-circuits corresponding to (almost uncoupled) σ^+ and σ^- polarization components. A growth of pump density involves two successive switch-ups, in the dominant σ^+ or σ^- component and then in the minor one [5, 6] (Fig. 1b).

The response diagram of a chiral system is more complicated. The most interesting solutions appear if ρ_p and $\delta_c = E_0^+ - E_0^-$ have opposite signs, i. e. if the pump polarization is biased towards that of the lower split-off polariton level. In this case each of the σ^\pm modes has its own advantage over the other: whilst the lower one is pumped more “intensively” (e.g. $|F_+| > |F_-|$), the upper one is closer to the resonance with the pump field that is blue-detuned from both. As a result, for a certain pump there may coexist three high-energy branches corresponding to σ^\pm components switched-up individually and in combination (Fig. 1c). Due to the same reason the intra-cavity

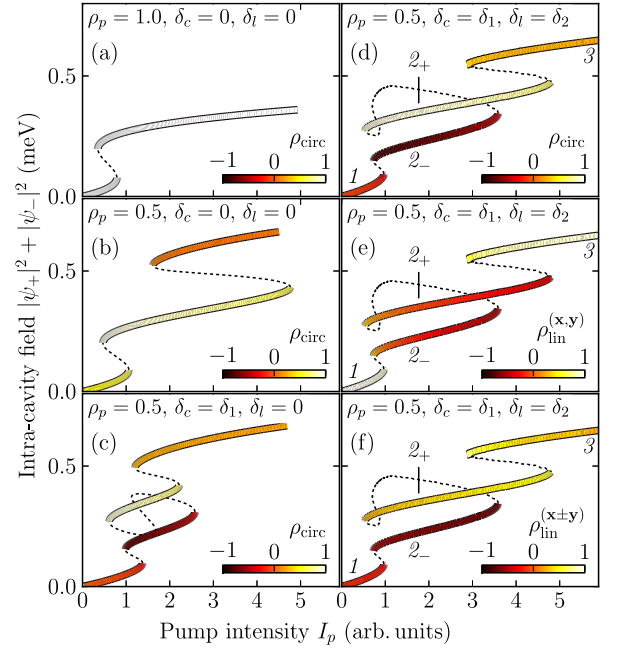


FIG. 1. (Color online) The steady-state response of the driven polariton mode, $|\psi_+|^2 + |\psi_-|^2$ vs. I_p , for several combinations of ρ_p , δ_c , and δ_l which are indicated at the top of each panel ($\delta_1 = -0.12 \text{ meV}$, $\delta_2 = 0.05 \text{ meV}$, $\Phi_p = 0$). The branches of asymptotically stable solutions are shown by colored heavy lines, the color indicates the degrees of circular polarization (a–d) and linear polarization in (x,y) basis (e) and (x+y, x–y) basis (f); unstable branches are shown by dashed lines.

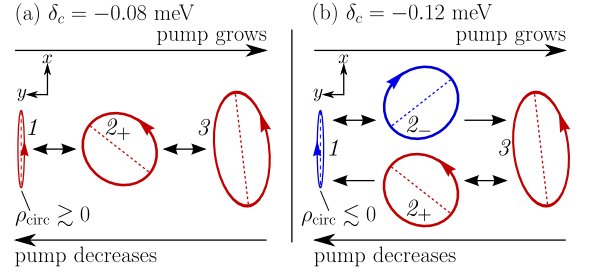


FIG. 2. (Color online) The scheme of non-equilibrium transitions in a chiral system with (a) $\delta_c = -0.08 \text{ meV}$ and (b) $\delta_c = -0.12 \text{ meV}$; in both cases $\delta_l = 0.05 \text{ meV}$, $\rho_p = 0.5$, $\Phi_p = 0$. Ellipses schematically represent the polarizations typical of the stability branches 1, 2_\pm , and 3 which are explicitly labeled in Fig. 1d–f.

circular polarization in the lowermost state can be either positive (right) or negative (left) depending on Δ and $\delta_{c,l}$.

Fig. 1d represents the system with $\rho_p = +0.5$, $\delta_c = E_0^+ - E_0^- = -0.12 \text{ meV}$, and $\delta_l = E_0^{(x)} - E_0^{(y)} = 0.05 \text{ meV}$; the main axis of pump polarization is x-directed, so that $\Phi_p = 0$. The X-Y splitting involves the mixing of the σ^\pm polarization components, which is sensitive to the phase difference of ψ_\pm . In the considered case it extends the range of I_p where only one of the σ^\pm components is found in the “up” position. If the sign of δ_l were negative

(or the pump polarization were y -directed), the region with the two highly polarized stability branches would be reduced.

Transitions between stability branches. In a degenerate system the order of the switch-ups is rigidly determined by the bias of pump polarization; the reverse transitions observed in the course of decreasing pump always proceed in the “last-up, first-down” order (Fig. 1b). In chiral systems, such a behavior takes place at small δ_c (Fig. 2a), but at larger δ_c a qualitatively distinct evolution scenario appears (Fig. 2b). Given the system starts from the lower stability branch (1) in Fig. 1d, a slowly increasing pump successively transfers it to branch 2_- (that is mainly σ^- polarized) and then to branch 3 [27]. However, the reverse transition $3 \rightarrow 1$ proceeds through the σ^+ -polarized branch 2_+ . Thus, the transitions occur in the “last-up, last-down” order that allows the cavity-field polarization to be inverted.

As shown by numerical simulations performed for 70 ps long pump pulses (see below), the system undergoes either $1 \rightarrow 2_+$ or $1 \rightarrow 2_-$ transformation depending on the sign of polarization (ρ_{circ}) in the low-energy state at branch 1 (Fig. 2). In other words, a small externally controlled right or left bias of *intra-cavity* polarization determines the branch the system jumps to on reaching the threshold pump power.

Experiment.—The sample has four 7 nm thick GaAs quantum wells separated by 4 nm AlAs barriers which are centered in a half- λ cavity. Its top (bottom) mirror consists of 32 (36) $\text{Al}_{0.2}\text{Ga}_{0.8}\text{As}/\text{AlAs}$ Bragg reflectors; GaAs substrate was etched in order to perform transmission measurements. The Q -factor is $7 \cdot 10^3$; the Rabi splitting and the exciton-photon detuning are 10.5 meV and $E_C - E_X(\mathbf{k}=0) \approx -5$ meV, respectively; the decay rate of the lower polariton state at $\mathbf{k}=0$ is $\gamma_0 \approx 0.05$ meV. The sample, placed into the magneto-optical cryostat at $T = 2$ K, is excited by optic pulses with a repetition rate of 8 MHz and duration of 70 ps generated by a mode-locked Ti:sapphire laser. The pump beam is directed along the cavity normal and focused into a $30 \mu\text{m}$ wide spot on the sample. The transmission signal is detected by a streak-camera with spatial and time resolutions of $7 \mu\text{m}$ and 6 ps, respectively. Under a weak excitation in zero magnetic field the cavity spectrum exhibits two linearly polarized levels separated by $\delta_l \approx 0.05$ meV.

To perform simulations, we solve numerically the many-mode Gross-Pitaevskii equations of type (1) [24] with a $30 \mu\text{m}$ wide Gaussian pump source; the model parameters nearly coincide with the experimental ones. In order to avoid complexity brought on by spatial inhomogeneity of the transmission (see [6, 8, 9]), below we only consider the time dependences of the signal collected from the spot center (in both the experiment and modeling). At last, in order to simulate finite time resolution and a partial weakly controlled time and space smoothing of the measured signal, the calculated intensities are

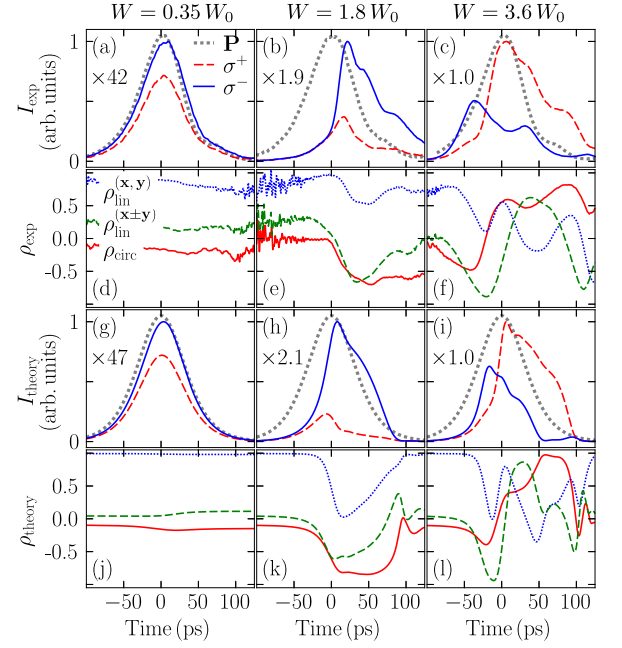


FIG. 3. (Color online) (a–c) Measured time dependences of the σ^+ (solid lines) and σ^- (dashed lines) components of the transmission signal at $\delta_c = -0.12$ meV; the pump shape is shown by heavy dotted lines. (d–f) The corresponding time dependences of the signal polarization in the circular basis (solid lines), (x, y) basis (dotted lines), and $(x \pm y)$ basis (dashed lines). Different columns correspond to different peak pump powers indicated at the top panels. (g–i) The modeled counterpart time dependences.

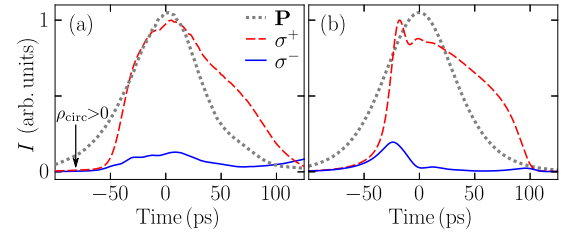


FIG. 4. (a) Measured and (b) calculated time dependences of the σ^+ and σ^- components of the transmission signal at $\delta_c = -0.08$ meV and $W = 3.6 W_0$.

averaged over the neighboring 10 ps in each time point.

Fig. 3 shows the dynamics of the system whose steady-state properties have been discussed in Figs. 1d–f. Most importantly, the pump polarization is biased towards the lower split-off circular polarization component ($\rho_p = +0.5$) and the upper linearly polarized eigenstate of a spin-degenerate system (the x direction). The Zeeman splitting $\delta_c \approx -0.12$ meV is involved by the magnetic field $B \approx 6$ T. The three basis polarization degrees of the signal, the circular one, ρ_{circ} , and two linear ones, $\rho_{\text{lin}}^{(x,y)}$ and $\rho_{\text{lin}}^{(x \pm y)}$, are shown in Figs. 3d–f, whereas Figs. 3a–c show only the circularly polarized components of the transmission intensity. Left column in Fig. 3 represents

the case of a low peak pump intensity $W = \max_t I_p(t) \approx 0.35W_0$, where W_0 corresponds to the first switch-up point in both the experiment and calculation; in the experiment, $W_0 \approx 500 \text{ kW/cm}^2$. In this case the signal polarization is nearly constant, though it does not coincide with that of the pump beam due to the splitting of polariton modes with different polarizations. In fact, the signal is almost linearly polarized with a slight bias towards σ^- according to Figs. 1d–f.

The middle column in Fig. 3 represents the above-threshold dynamics at $W = 1.8W_0$; a 5-fold increase in W involves more than a 20-fold increase in the transmission signal (compare Figs. 3a,b). The signal appears to be mainly σ^- -polarized, and nearby the peak excitation it also exhibits a prominent polarization in the “diagonal” ($\mathbf{x} - \mathbf{y}$) direction (see Fig. 3e). This makes up a clear manifestation of the $1 \rightarrow 2_-$ transition (Fig. 1f).

A further two-fold increase in W up to $3.6W_0$ (right column in Fig. 3) allows us to track the double $1 \rightarrow 2_- \rightarrow 3$ transition proceeding during the growth of pump density [27] as well as the “asymmetric” reverse transition $3 \rightarrow 2_+$ at the back front of the pulse, which are schematically shown in Fig. 2b. In particular, according to Fig. 3c the signal exhibits first the switch-up in the σ^- component (leading to high negative values of ρ_{circ}) and next, with increasing pump, the switch-up in σ^+ (so that ρ_{circ} becomes positive). Finally, the switch-down in σ^- at the back front results in a further growth of ρ_{circ} up to the values exceeding the pump polarization. The transitions observed in all the three basis polarizations agree with the simulation shown in Fig. 3i,l and conform to the steady-state diagram in Fig. 1d–f. According to the latter, (i) $\rho_{\text{lin}}^{(\mathbf{x}\pm\mathbf{y})}(t)$ exhibits the sign reversal during the $2_- \rightarrow 3$ transition and (ii) $\rho_{\text{lin}}^{(\mathbf{x},\mathbf{y})}(t)$ has two minima, of which the first is immediately before the $2_- \rightarrow 3$ transition ($t \approx -20 \text{ ps}$) and the second is immediately after the $3 \rightarrow 2_+$ transition ($t \approx +50 \text{ ps}$).

The discussed transitions differ from those in a system with small δ_c splitting. A typical dynamics in a 1.5 times smaller magnetic field ($B = 4 \text{ T}$, so that $\delta_c = -0.08 \text{ meV}$, and $W = 3.6W_0$) is presented in Fig. 4. Its main distinction is a positive sign of the signal polarization in a low-energy state ($\rho_{\text{circ}} > 0$ at $t < -60 \text{ ps}$) like that in the pump field, which predetermines the $1 \rightarrow 2_+$ trajectory under increasing pump power. A further increase in W (not shown) involves the $2_+ \rightarrow 3$ transition. In fact, this scenario, representing a steady-state scheme in Fig. 2a, is qualitatively the same as that predicted [5] and observed [8] for a spin-degenerate system. However, our system is not affected by the long-lived excitonic reservoir (see Ref. [13, 28]) due to a comparatively short duration of pump pulses. Indeed, in the opposite case or in a case of a large positive V_2 the switch-up in the “leading” σ^+ or σ^- component would force the minor one to increase as well due to the blueshift, so that a high circular polar-

ization well above the threshold would be unreachable.

To summarize, we have discovered a novel mechanism of fast cavity-field polarization conversion from mainly σ^- to σ^+ states or vice versa due to varying pump intensity, which can be implemented in chiral cavities or photonic crystals with energy-split σ^\pm polariton eigenstates. Its physical prerequisite is that the blue-shift of a resonance can be larger than its spectral linewidth, which is achieved due to the strong light-matter coupling. This effect can be used in the future highly tunable optic switchers and logic elements working in the picosecond range or for creating short light pulses with rapidly changing polarization.

The authors are grateful to V.B. Timofeev and S.G. Tikhodeev for fruitful discussions. This work was supported by the RF President grant MK-6863.2012.2, RFBR, and the State of Bavaria.

* gavr_ss@issp.ac.ru

- [1] C. Weisbuch *et al.*, Phys. Rev. Lett. **69**, 3314 (1992).
- [2] R. M. Stevenson *et al.*, Phys. Rev. Lett. **85**, 3680 (2000).
- [3] J. I. Inoue, T. Brandes, and A. Shimizu, Phys. Rev. B **61**, 2863 (2000).
- [4] R. Takayama *et al.*, Eur. Phys. J. B **25**, 445 (2002).
- [5] N. A. Gippius *et al.*, Phys. Rev. Lett. **98**, 236401 (2007).
- [6] I. A. Shelykh, T. C. H. Liew, and A. V. Kavokin, Phys. Rev. Lett. **100**, 116401 (2008).
- [7] T. C. H. Liew, A. V. Kavokin, and I. A. Shelykh, Phys. Rev. Lett. **101**, 016402 (2008).
- [8] D. Sarkar *et al.*, Phys. Rev. Lett. **105**, 216402 (2010).
- [9] C. Adrados *et al.*, Phys. Rev. Lett. **105**, 216403 (2010).
- [10] T. K. Paraíso *et al.*, Nat Mater **9**, 655 (2010).
- [11] D. N. Krizhanovskii *et al.*, Phys. Rev. B **77**, 115336 (2008).
- [12] A. A. Demenev *et al.*, Phys. Rev. Lett. **101**, 136401 (2008).
- [13] S. S. Gavrilov *et al.*, Phys. Rev. B **85**, 075319 (2012).
- [14] M. Sich *et al.*, Nat Photon **6**, 50 (2012).
- [15] M. I. Dykman and A. L. Velikovich, Opt. Commun. **70**, 151 (1989).
- [16] T. Ackemann and M. Sondermann, APL **78**, 3574 (2001).
- [17] T. Mori, Y. Yamayoshi, and H. Kawaguchi, APL **88**, 101102 (2006).
- [18] K. Konishi *et al.*, Phys. Rev. Lett. **106**, 057402 (2011).
- [19] A. Armitage *et al.*, Phys. Rev. B **55**, 16395 (1997).
- [20] R. B. Balili *et al.*, APL **88**, 031110 (2006).
- [21] P. Renucci *et al.*, Phys. Rev. B **72**, 075317 (2005).
- [22] K. V. Kavokin *et al.*, Phys. Stat. Sol. (c) **2** (2005).
- [23] M. Vladimirova *et al.*, Phys. Rev. B **82**, 075301 (2010).
- [24] S. S. Gavrilov *et al.*, JETP **110**, 825 (2010).
- [25] A. Baas *et al.*, Phys. Rev. A **69**, 023809 (2004).
- [26] N. A. Gippius *et al.*, EPL **67**, 997 (2004).
- [27] A direct $2_- \rightarrow 2_+$ transition, which might seem possible according to Fig. 1d, does not happen unless branch 2_+ became the single available branch in a finite range of I_p ; this would be the case for sufficiently larger δ_l values than that considered in our work
- [28] S. S. Gavrilov *et al.*, JETP Lett. **92**, 171 (2010).